



Identification and validation of expressed HLA-binding breast cancer neoepitopes for potential use in individualized cancer therapy

Hannah Reimann,¹ Andrew Nguyen,² J Zachary Sanborn,² Charles J Vaske,³ Stephen C Benz,² Kayvan Niazi,³ Shahrooz Rabizadeh,³ Patricia Spilman ³, Andreas Mackensen,¹ Matthias Ruebner,⁴ Alexander Hein,⁴ Matthias W Beckmann,⁴ Edith D van der Meijden,¹ Judith Bausenwein,¹ Sascha Kretschmann,¹ Marieke Griffioen,⁵ Jeffrey Schlom,⁶ James L Gulley ⁷, Karin L Lee,⁶ Duane H Hamilton,⁶ Patrick Soon-Shiong,³ Peter A Fasching,⁴ Anita N. Kremer¹

To cite: Reimann H, Nguyen A, Sanborn JZ, *et al.* Identification and validation of expressed HLA-binding breast cancer neoepitopes for potential use in individualized cancer therapy. *Journal for ImmunoTherapy of Cancer* 2021;**9**:e002605. doi:10.1136/jitc-2021-002605

► Additional supplemental material is published online only. To view, please visit the journal online (<http://dx.doi.org/10.1136/jitc-2021-002605>).

HR and AN are joint first authors.

PAF and ANK are joint senior authors.

Accepted 10 May 2021



© Author(s) (or their employer(s)) 2021. Re-use permitted under CC BY-NC. No commercial re-use. See rights and permissions. Published by BMJ.

For numbered affiliations see end of article.

Correspondence to

Patricia Spilman;
patricia.spilman@immunitybio.com

ABSTRACT

Background Therapeutic regimens designed to augment the immunological response of a patient with breast cancer (BC) to tumor tissue are critically informed by tumor mutational burden and the antigenicity of expressed neoepitopes. Herein we describe a neoepitope and cognate neoepitope-reactive T-cell identification and validation program that supports the development of next-generation immunotherapies.

Methods Using GPS Cancer, NantOmics research, and The Cancer Genome Atlas databases, we developed a novel bioinformatic-based approach which assesses mutational load, neoepitope expression, human leukocyte antigen (HLA)-binding prediction, and in vitro confirmation of T-cell recognition to preferentially identify targetable neoepitopes. This program was validated by application to a BC cell line and confirmed using tumor biopsies from two patients with BC enrolled in the Tumor-Infiltrating Lymphocytes and Genomics (TILGen) study.

Results The antigenicity and HLA-A2 restriction of the BC cell line predicted neoepitopes were determined by reactivity of T cells from HLA-A2-expressing healthy donors. For the TILGen subjects, tumor-infiltrating lymphocytes (TILs) recognized the predicted neoepitopes both as peptides and on retroviral expression in HLA-matched Epstein-Barr virus-lymphoblastoid cell line and BC cell line MCF-7 cells; PCR clonotyping revealed the presence of T cells in the periphery with T-cell receptors for the predicted neoepitopes. These high-avidity immune responses were polyclonal, mutation-specific and restricted to either HLA class I or II. Interestingly, we observed the persistence and expansion of polyclonal T-cell responses following neoadjuvant chemotherapy.

Conclusions We demonstrate our neoepitope prediction program allows for the successful identification of neoepitopes targeted by TILs in patients with BC, providing a means to identify tumor-specific immunogenic targets for individualized treatment, including vaccines or adoptively transferred cellular therapies.

BACKGROUND

Cancer therapies based on immunological approaches are rapidly becoming standard for many cancer types.^{1–4} In particular, immunological checkpoint inhibitors such as cytotoxic T-lymphocyte associated protein 4 (CTLA-4), programmed death ligand 1 (PD-L1) and programmed death protein 1 (PD-1) antibodies are gaining approval for the treatment of a growing number of cancer types; however, they have shown little clinical efficacy in breast cancer (BC), with response rates of 20%–25% in previously untreated cases of advanced triple-negative breast cancer (TNBC) and 5%–10% in pretreated patients; nonetheless, when efficacy is seen, it is often durable. Larger phase III trials for checkpoint inhibitors in BC are under way.^{5,6} Results have been more promising for combination chemotherapy and immune checkpoint therapy as shown by the recent Food and Drug Administration and European Medicines Agency approval of use of the PD-L1 inhibitor atezolizumab in combination with nab-paclitaxel as first-line therapy for metastasized or unresectable locally advanced TNBC.⁷ However, there continues to be a large unmet clinical need for the development of effective immunotherapies for the treatment of BC.

Expansion and subsequent adoptive transfer of large numbers of tumor-infiltrating lymphocytes (TILs)^{8,9} have been shown to be effective in treating some cancers, demonstrating the clinical potential for individualized immune therapies. However, current strategies largely rely on non-specific

expansion and reinfusion of TILs without identification and isolation of tumor-specific T cells. Neopeptides are epitopes created by non-synonymous mutations in the tumor genome. As these mutations are restricted to the tumor, neopeptides can induce high-avidity mutation-specific T-cell responses. In contrast, tumor-associated antigens, which are purely overexpressed in the tumor as compared with healthy tissue, often fail to induce high-avidity T-cell responses as these T cells are largely depleted during thymic development. Mutation-specific targeting of the tumor is also less likely to induce autoimmunity. Here we establish a feasible cancer neopeptide discovery and validation program that can inform the development of patient-specific neopeptide-targeted therapies using either adoptively transferred neopeptide-specific TILs or neopeptide-targeted therapeutic vaccines.

Previously, to establish our method, we used GPS Cancer,¹⁰ NantOmics research (including several breast cancer samples), and The Cancer Genome Atlas (TCGA) databases (dbs) by whole-genome sequencing (WGS) data and RNA sequencing (RNA-Seq) data for 750 patients with cancer across 23 cancer classifications, to identify neopeptides, to determine whether recurrent neopeptides were prevalent in invasive BC, and to identify those neopeptides that may be capable of binding to the HLA. We have previously used this program to identify neopeptides in the clinical trial QUILT 2.025 (NCT03552718).

These techniques were refined and tested experimentally using the well-characterized human breast carcinoma basal-type triple-negative cell line, MDA-MB-231.^{11 12} Because MDA-MB-231 cells express the HLA-A2 restriction element, we were able to use established assays to compare the *in silico* predicted HLA-A2 binding of potential neopeptides to *in vitro* binding assays. This allowed us to directly assess the efficacy by which binding algorithms can accurately predict peptides capable of being presented by a patient's HLA. Using the cell line, we confirmed the feasibility of the pipeline. We then demonstrated its clinical feasibility in two patients with BC enrolled on the Tumor-Infiltrating Lymphocytes and Genomics (TILGen) study.^{13 14}

PATIENT SAMPLES AND METHODS

Neopeptide prediction and prioritization by successive filtering using genomics, transcriptomics and HLA typing

To predict specific neopeptides, we established an analysis workflow pipeline. It starts with genomic analysis to identify possible neopeptides, followed by expression analysis and further HLA-binding prediction to narrow an initial large set of possible neopeptides down to those most likely to be actionable. As an example of this, for 26 patients with TNBC, we identified single-nucleotide variants (SNVs) and insertions/deletions (INDELs) as previously described¹⁵ using TCGA WGS. Tumor mutational burden (TMB) was determined as part of these analyses, and the results reported here are based, in part, on data

generated by the TCGA Research Network (<https://www.cancer.gov/tcga>).

Genomic analysis was followed by RNA-Seq-based expression determination. For these analyses, tumor tissue data were compared with germline data. This filtering step eliminates all non-expressed possible neoantigens.

After filtering by WGS and RNA-Seq data, potential neopeptides underwent HLA-binding prediction to further reduce the pool of potentially actionable neopeptides.

Since HLA class I alleles predominantly bind to 9-mer peptide fragments,^{16 17} we chose to focus on the identification of 9-mer neopeptides. Neopeptides were identified by windowing around all possible 9-mer amino acid sequences derived from an identified non-silent SNV or INDEL. As a means to reduce possible off-target effects of a particular neopeptide, we filtered all identified neopeptides against all possible 9-mer (HLA class I epitopes) and 15-mer peptide (HLA class II epitopes) sequences created from every known human gene using the reference human genome. These epitopes represent the normal epitopes that the immune system should 'ignore'; that is, they should not provoke an immune response. In addition, we added single-nucleotide polymorphisms (SNPs) from the db for SNPs (<http://www.ncbi.nlm.nih.gov/SNP/>) to account for rare protein sequences that we may have missed within the sequencing data. Neopeptides were ranked by RNA expression based on RNA-Seq data as well as the allele frequency of the observed coding variant to offset issues arising from tumor heterogeneity, a method we used previously as part of a study of vaccines in murine tumor models.¹⁸

HLA typing

HLA typing was performed by aligning sequencing reads to the ImMunoGeneTics/HLA db.¹⁹ HLA alleles were scored by a sum of coverage of sequencing over the entire HLA gene region and the amount of sequencing reads (depth) over the region as well as alignment scores. Highest scores were determined to be the correct HLA sequence.

Neopeptide–HLA binding affinity

NetMHC 3.4 (<http://www.cbs.dtu.dk/services/NetMHC-3.4/>)^{20–22} was used to predict whether a neopeptide would bind to a specific HLA allele. In general, neopeptides with predicted binding affinities of <500 nM protein concentration underwent further analysis in the MDA-MB-231 and TILGen patient studies.

Neopeptide identification pipeline applied to the MDA-MB-231 BC cell line

The neopeptide identification method described previously for TCGA data was then applied to the MDA-MB-231 BC cell line,^{11 12} starting with sequencing and genomic analysis, with focus on HLA-A2. Thereby, 50 potential neopeptides predicted to bind HLA-A2 were identified. Of these, 20 were synthesized for testing of HLA-A2

binding (online supplemental table S1), which was determined by incubation of neoantigen peptides with T2A2 cells²³ and assessment of affinity by flow cytometry.

Cytotoxic T-lymphocyte lysis assays

For use in cytotoxic T-lymphocyte assays, neoepitope-specific HLA-A2-expressing T cells, dendritic cells (DCs), and ultimately CD8+ cells from peripheral blood mononuclear cells (PBMCs) donated by healthy individuals were generated (method details in the online supplemental file).

Purified, stimulated CD8+ cells were used in a lysis assay using MDA-MB-231 (BC) or SW620 colon cancer cells^{24,25} as targets to assess specificity of the predicted neoantigens for a cancer tissue type. Targets were labeled with carboxyfluorescein succinimidyl ester and plated at 3000 cells/well (in 100 μ L). Effector cells were added to targets at various effector:target ratios (in triplicate). Where indicated, target cells were incubated with either anti-HLA-A2 or control IgG antibodies (One Lambda) for 2 hours at 37°C prior to the addition of effector T cells. Assays were incubated overnight at 37°C. Following incubation, dead cells were stained with propidium iodide (1 μ g/mL final concentration) and analyzed on a Celigo Imaging Cytometer (Nexcelom). Percent cell death is defined as $(1 - (\text{livesample} / \text{livespontaneous})) \times 100$.

Preclinical validation of neoepitope prediction in patients with BC

Collection of peripheral blood and tumor tissue for analysis

Subsequently, we applied our neoepitope prediction method to samples from two subjects in the TILGen study.¹³ A brief description of the study and methods for peripheral blood and tumor tissue collection and analysis are presented in the online supplemental file. TILGen patient 1 had HER2+ BC and TILGen patient 2 had TNBC; both received neoadjuvant chemotherapy and had pathological complete remissions. The patients' diagnoses were based on immunohistochemical (IHC) analysis rather than gene expression profiling to facilitate our workflow wherein the isolation of TILs requires rapid diagnosis.

Peripheral blood and tumor tissue were obtained after approval by the internal Institutional Review Board (IRB) and with informed patient consent according to the Declaration of Helsinki. Peripheral blood was used for isolation of germline DNA, antigen-presenting B cells to be immortalized with Epstein-Barr virus (EBV) to generate lymphoblastoid cell lines (LCLs),²⁶ and monocyte-derived DCs (details in the online supplemental file or in Patient samples and methods). TILs were isolated from tumor tissue to generate the T-cell clones used for culture experiments as described further and in the online supplemental file.

Selection of TILGen peptides for synthesis

After sequencing the tumor and normal genome of the TILGen subjects, determination of possible neoepitopes,

and filtering transcriptomic analyses, peptides were selected for synthesis based on predicted HLA affinity. Synthetic peptides for the predicted neoepitopes were obtained at purity above 70% from GeneCust (Luxembourg). For HLA class I, all predicted peptides were synthesized as 9-mers. For HLA class II, all neoepitopes comprising the same mutation were fused to one long peptide ranging from 15 to 29 amino acids (online supplemental tables S2 and S3).

Expansion and isolation of TILs

TILs were expanded from patient tumor tissue and cell culture experiments performed with TILGen subject samples to determine neoepitope recognition. Biopsies obtained from the two TILGen patients were cultured in Roswell Park Memorial Institute (RPMI) with 40 U/mL penicillin/streptomycin, 2 mM L-glutamine, 50 μ M β -mercaptoethanol (all Gibco), and 5% fetal calf serum (FCS), 5% human serum, 0.4% vitamin solution, 1% minimal essential medium, and 1 mM sodium pyruvate (all PAN-Biotech, Germany) in the presence of 2.5×10^5 CD3/CD28 beads/mL (Gibco), 100 U/mL IL-2 (Proleukin) and 5 ng/mL IL-15 (Cellgenix, Germany) for 14–21 days.

Antigen presentation assays for BC-derived neoepitopes

EBV-LCLs and DCs were used as autologous antigen-presenting cells (APCs), HeLa cells after transduction with HLA molecules to determine HLA-restriction, and MCF-7 cells transduced with the respective HLA molecule and with neoepitopes or wild-type (wt) counterparts for processing and presentation assays.

EBV-LCL, HeLa and MCF-7 cells were cultured in RPMI with the same additives as described previously for TILs, but with 10% FCS. The T-cell clones were cultured in RPMI also with the same additives but 5% human serum, 5% FCS and 200 IU/mL IL-2, and were restimulated every 10–20 days with irradiated allogeneic PBMCs and 0.8 μ g/mL phytohemagglutinin (Thermo Scientific).

Autologous DCs of the two patients with BC were generated from monocytes isolated from autologous PBMCs by magnetic separation as described in the online supplemental data.

Expanded T-cell lines were cocultured with autologous EBV-transformed LCLs (EBV-LCLs) or autologous DCs loaded with a peptide pool (1 μ g/mL) of potential neoepitopes at an effector:target ratio of 4:1. Activated T cells were clonally isolated by flow cytometric cell sorting after 4.5 hours (interferon gamma (IFN- γ) secretion assay, Miltenyi Biotec) or 36 hours (CD137 expression determined by flow cytometry).

The stimulator cells (5×10^4 cells/well), including EBV-LCL, HeLa or MCF-7 cultured in RPMI with 10% FCS, were coincubated overnight in U-bottom 96-well plates with T-cell clones (5×10^3 cells/well), which were expanded after peptide stimulation from patient-derived TILs. Details of peptide pulsing can be found in the online supplemental data.

Retroviral transduction of neoantigens and HLA alleles, flow cytometry, T-cell receptor (TCR) sequencing, and clonotypical PCR

To confirm natural processing and presentation of neoantigens occurs after endogenous expression, sequences for the neoantigens were cloned into retroviral vectors for the transduction of EBV-LCL, HeLa or MCF-7 cells as described in the online supplemental file.

Methods for flow cytometry for either analysis or isolation of cells using labeling with CD3 (fluorescein isothiocyanate/FITC or Brilliant Violet 510/BV510), APC-Cy7 or APC CD8, BV421 CD4, PE CD137 and NGFR are detailed in the online supplemental file.

TCR sequencing of T-cell clones, and clonotypical PCR, including all plasmids and oligonucleotides used for cloning (online supplemental table S4), are described in the online supplemental file.

RESULTS

Successive filtering by neopeptide burden, expression, and HLA binding leads to identification of high-probability actionable neopeptides in TCGA TNBC cases

Analysis of TCGA data revealed that successive elimination of potential TNBC neopeptides first identified by WGS sequencing for SNVs and INDELs, then filtered for RNA expression levels and finally potential HLA class I binding—as well as similarity to peptide sequences present elsewhere within the normal human proteome—eliminates the vast majority of potentially targetable mutations (figure 1A). This successive filtering allows prioritization of potential neopeptides with the highest probability for being actionable for further testing.

HLA-A2 binding and ability to activate T cells further narrow actionable neopeptides

To test the reactivity of T cells to neoantigen candidates in vitro, we used our bioinformatics-based neopeptide identification method that includes sequencing to identify 50 potential neopeptides in the MDA-MB-231 human BC cell line predicted to bind to HLA-A2. A library of 20 peptides was synthesized, comprising the top 14 based on predicted HLA-A2 binding affinity, the top 6 based on expression levels, and 6 peptides whose low expression levels or poor predicted HLA-A2 binding would presumably make them less than ideal candidates for immunological targeting (online supplemental table S1). We synthesized 20 of these potential neopeptides and found that 7 of 20 were capable of binding HLA-A2 in vitro (figure 1B). Using peripheral blood from normal HLA-A2 human donors, we screened five peptides for their ability to expand reactive T cells. One identified neopeptide, SLC17A5 (GTIGIFWFV), was able to expand reactive T cells in all normal donors assayed (figure 1C). These SLC17A5-reactive T cells were capable of specifically lysing the MDA-MB-231 BC cell line in an HLA-A2-restricted manner (figure 1D,E).

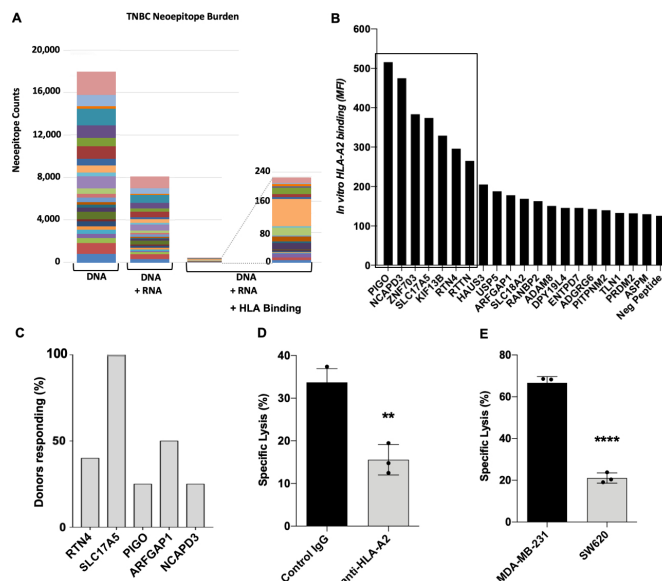
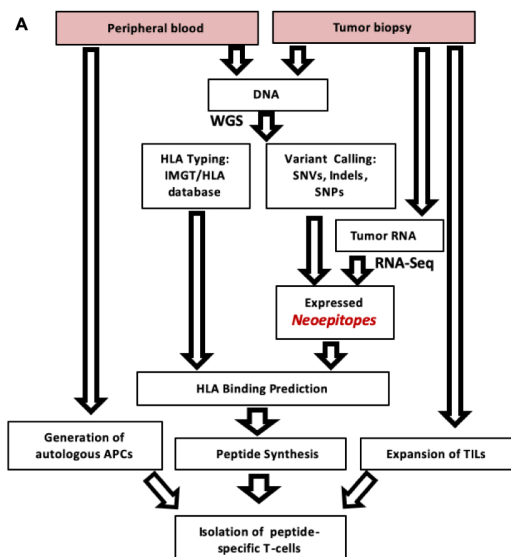


Figure 1 Potentially actionable neopeptides are filtered by sequential DNA/RNA/HLA analyses. (A) Within the TNBC TCGA dataset filtered by WGS (DNA), then expression (RNA) and finally HLA-binding prediction (HLA); the final set of actionable neopeptides showed no recurrent mutations. Different colors represent individual patient samples. (B) Application of DNA/RNA/HLA neopeptide filtering to MDA-MB-231 cell line resulted in identification of 50 potential HLA-A2-binding neopeptides, synthesis of 20 9-mer neopeptides, and determination of HLA-A2 binding using T2A2 cells revealed seven peptides with good binding (boxed, MFI>200). (C) Percentage of normal HLA-A2 donors responding by expansion of reactive T cells to five potential neopeptides indicates SLC17A5 elicited a response from all donors (n=4–6 normal donors per peptide). (D) Lysis of MDA-MB-231 cells by SLC17A5-reactive T cells is blocked by an anti-HLA-A2 antibody. (E) Lysis of MDA-MB-231 and SW620 cells by SLC17A5-reactive T cells is greater for the BC cell line. Statistics performed using an unpaired Student's t-test; **p<0.01, ****p<0.0001. MFI, Mean Fluorescence Intensity; TCGA, The Cancer Genome Atlas; TNBC, triple-negative breast cancer; WGS, whole-genome sequencing.

Neopeptide prediction and validation for two patients with TILGen BC

An expanded neopeptide identification pipeline comprising HLA-binding prediction for HLA class I and II molecules of the respective patients was used for two TILGen subjects as shown in figure 2A. TILGen 1 was a patient with HER2+ BC and TILGen 2 was a patient with TNBC. Receptor status information was known previous to this study. WGS of these tumor samples revealed a higher TMB for subject 2, and comparison to corresponding reference DNA revealed 68 and 274 non-synonymous mutations, respectively (figure 2B). Based on genomic analysis only, 206 and 964 neopeptides were predicted for subjects 1 and 2, respectively, but RNA-Seq expression analysis decreased this to 143 and 809; HLA class I binding prediction narrowed it further to 20 for subject 1 and 26 for subject 2; HLA class II binding prediction added another 8 for patient 1 and 39 for patient 2; see the



Pt #	TMB	Non-Syn. SNV	HR Status	Predicted Neoepi.	Neoepitopes filtered by:	
					Expression	Expression & HLA Class I Binding
1	2.85	68	ER+/PR+/Her2+	206	143	20
2	11.6	274	ER-/PR-/Her2-	964	809	26

Figure 2 Analysis workflow for neoepitope identification in TILGen subjects and subject genomic and expression information. (A) In the proposed workflow, WGS is performed on DNA from both peripheral blood and patient tumor biopsies for HLA typing, variant calling, and binding prediction; tumor RNA-Seq analysis is used to confirm expression. Autologous APCs are generated from peripheral blood, and TILs are expanded from tumor tissue. Peptides with confirmed expression and predicted binding to a patient HLA class I or II molecule are then synthesized and used for isolation of peptide-specific T cells. (B) When this workflow was applied to the two TILGen subjects, WGS-based TMB was found to be higher in subject 2, as were non-synonymous SNVs; both predicted neoepitopes and number of expressed potential neoepitopes were higher in subject 2. Hormone receptor status for these subjects was previously determined as part of the TILGen study, not the workflow shown here. APC, antigen-presenting cell; ER, estrogen receptor; HER2, human epidermal growth factor receptor 2; IMGT, ImMunoGeneTics; PR, progesterone receptor; RNA-Seq, RNA sequencing; SNP, single-nucleotide polymorphism; SNV, single-nucleotide variant; TIL, tumor-infiltrating lymphocyte; TILGen, Tumor-Infiltrating Lymphocytes and Genomics; TMB, tumor mutational burden; WGS, whole-genome sequencing.

list of potential neoepitopes for patients 1 and 2 in online supplemental tables S2 and S3, respectively.

T-cell recognition of predicted neoantigens further refines actionable targets

The existence of TILs that recognize a neoantigen peptide further validates the neoantigen predicted by the workflow pipeline as likely actionable. To identify neoepitope-specific TILs, T cells were expanded from tumor biopsies of the two patients with BC. Expanded TILs were co-cultured with autologous EBV-LCLs or DCs

loaded with a pool of peptides encoding the predicted neoepitopes for each patient. T cells were then sorted based on expression of either the activation marker CD137 or secretion of IFN- γ , and clonally expanded. Growing T-cell clones were retested for recognition of autologous EBV-LCL pulsed with the individual patient-specific peptide pool by IFN- γ ELISA as shown for TILGen patient 2 in figure 3A.

All clones that were not reactive against the unpulsed EBV-LCL but strongly recognized autologous EBV-LCL loaded with the peptide pool were further analyzed by first testing recognition of subpools of the peptides and finally individual peptides. Matrix subpools enable fast identification of the targeted epitope while consuming minimal amounts of material. Subpools were generated from each patient-specific peptide pool wherein each peptide was present in three subpools. Based on the combination of recognized subpools, the individual peptide could be identified.

Among TILs derived from TILGen patient 2, we were able to identify 31 CD8+ and one CD4+ T-cell clones recognizing the peptide pools. We note again for the TILGen subjects, neoepitope prediction was based on binding to both class I and II HLA molecules. All of the CD8+ T-cell clones and the CD4+ T-cell clone of this patient were derived from screening for secretion of IFN- γ . While three of the CD8+ T-cell clones could not be further expanded, the other 28 specifically recognized a mutated variant of PNMAL1 (P100R) as shown in figure 3B. The CD4+ T-cell clone specifically recognized a mutated variant of CARS2 (Q171H) (figure 3C and online supplemental figure S1A,B).

From TILGen patient 1, we characterized three CD4+ T-cell clones (3E1, E15 and G44), with all three recognizing the mutated variant of the X-chromosomally encoded RNA-binding motif protein RBMX (T55I) (figure 3D and online supplemental figure S1C,D).

Specificity for the mutated variants—PNMAL1 (P100R) and CARS2 (Q171H) for TILGen patient 2 and RBMX (T55I) for TILGen patient 1—was confirmed by a lack of recognition of the wt alleles (figure 3B–D, respectively; additional clones are shown in the online supplemental figure S2). At the peptide concentrations used (0.01, 0.1, and 1 μ g/mL), the wt versions of PNMAL1 and RBMX neoepitopes did not stimulate the T-cell clones (figure 3E,G, respectively). The wt CARS2 neoepitope did stimulate the T-cell clones at 0.1 and 1 μ g/mL (figure 3F), but the mutated variant CARS2 induced much stronger T-cell recognition.

To ensure the identified neoepitopes are naturally processed and presented, we transduced HLA-matched EBV-LCL cells to express either the full length wt or mutated protein. T cells were capable of specifically recognizing the endogenously expressed mutated but not wt proteins (figure 3H–J).

These studies validate the predicted neoantigens RBMX for TILGen patient 1 and PNMAL1 and CARS2 for TILGen patient 2 as potentially actionable.

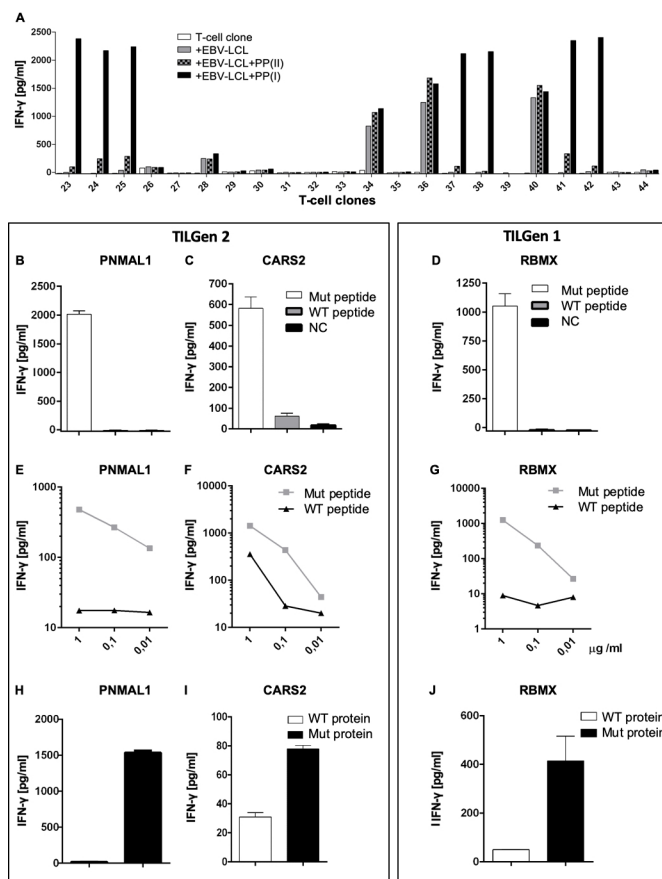


Figure 3 Identification of neopeptide-specific T-cell clones from BC biopsies, specificity and validation of natural processing. (A) Clonally expanded TILs from TILGen patient 2 were retested for recognition of the patient-specific HLA class I and HLA class II PP I/PP II by measuring IFN- γ secretion after stimulation with peptide-loaded autologous EBV-LCL in ELISA. Clones 23, 24, 25, 37, 38, 41, and 42 display specific recognition of the HLA class I peptide pool. For each identified neopeptide from TILGen subject 2 (B,C) or TILGen 1 (D), the Mut and wt variants of the peptides are tested for T-cell recognition after loading on autologous EBV-LCL as reflected by IFN- γ secretion. Representative T-cell clones for each antigen are shown: PNMAL1 clone 21 and CARS2 clone 55 (TILGen 2) and RBMX clone 3E1 (TILGen 1). Depicted are mean and SEM of triplicates. NC: unloaded autologous EBV-LCL. (E–G) T-cell recognition of Mut and wt peptides at decreasing concentrations as measured by IFN- γ ELISA is shown. Depicted are mean and SEM of duplicates. (H–J) T-cell recognition of retrovirally expressed full-length wt and Mut neoantigen proteins in HLA-matched EBV-LCL as measured in IFN- γ ELISA. Means and SEM of triplicates (PNMAL1) and of duplicates (RBMX and CARS2) are shown. BC, breast cancer; EBV, Epstein-Barr virus; IFN- γ , interferon gamma; LCL, lymphoblastoid cell line; PNMAL1, paraneoplastic Ma antigen family-like 1; CARS, cysteinyl tRNA synthetase 2; RBMX, RNA binding motif protein X-linked; Mut, mutated; NC, negative control; PP, peptide pool; TIL, tumor-infiltrating lymphocyte; TILGen, Tumor-Infiltrating Lymphocytes and Genomics; WT, wild type.

Polyclonal T-cell responses to PNMAL1 and RBMX

To differentiate between a polyclonal T-cell response against the identified neopeptides and repetitive detection of the same expanded T cells, we analyzed expression of the variable β -chain of the TCR (TILGen 2) or sequenced the CDR3 region of the TCR (TILGen 1) and observed that both PNMAL1 and RBMX elicited polyclonal T-cell responses (figure 4). This finding was supported by data obtained by testing truncated versions of the RBMX T55I. We observed that the minimal epitope of the recognized RBMX T55I peptide was shifted by one amino acid to the N-terminus or C-terminus among the different T-cell clones, but all required a core of seven to eight amino acids (online supplemental figure S3).

These data confirm polyclonal T-cell responses to RBMX for TILGen patient 1 and to PNMAL1 for TILGen patient 2, indicating the immunogenicity of these neopeptides.

Identified neopeptides were patient-specific

To determine whether or not the neopeptides we identified for TILGen patients 1 and 2 were frequently expressed in other patients with BC or were patient-specific, we analyzed 360 genomes from patients with BC, including 39 of the TILGen study, and were not able to find these mutations in any other patient, indicating that these neopeptides are truly patient-specific.

Characterization of HLA class II-restricted neopeptides

The RBMX T55I neopeptide identified in TILGen 1 was predicted to bind to three of the patient's HLA class II

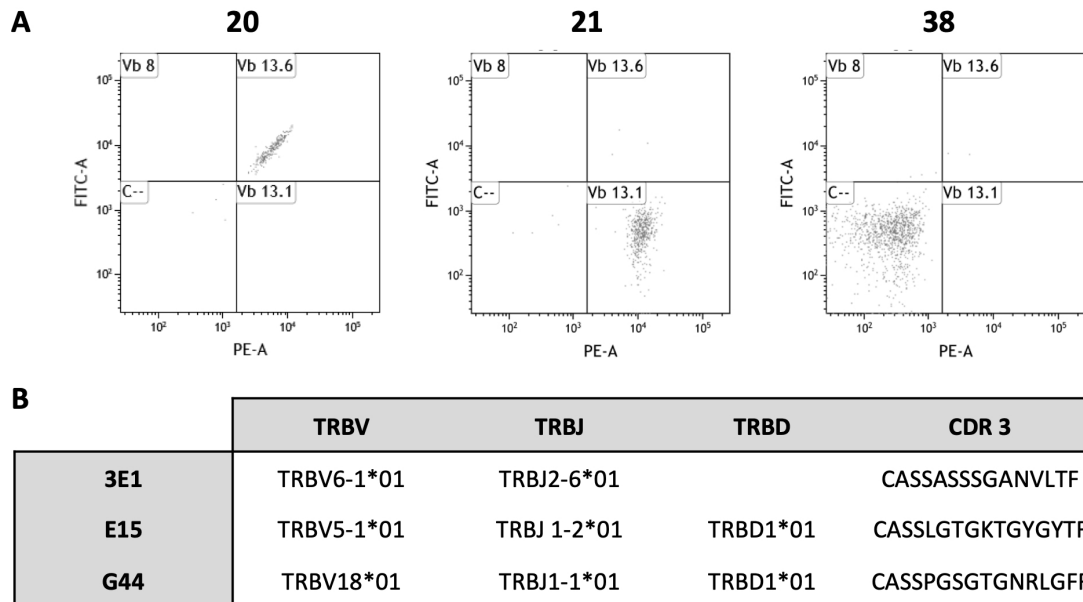


Figure 4 PNMA1 P100R- and RBMX T55I-elicited polyclonal immune responses. (A) Flow cytometric analysis of $\nu\beta$ chain usage of three exemplary PNMA1 P100R-specific T-cell clones is shown. (B) T-cell receptor sequencing of all three RBMX T55I-specific CD4+ T-cell clones demonstrated differential $\nu\beta$ chains and unique CDR3 regions. $\nu\beta$, variable beta; FITC, fluorescein isothiocyanate; TRBV, T-cell receptor beta-chain variable; TRBJ, T-cell receptor beta joining; and TRBD, T-cell receptor beta-chain diversity genes.

alleles (HLA-DRB1*15:01, HLA-DPB1*02:01 and HLA-DPB1*04:01, respectively). To characterize the HLA restriction of these RBMX T55I-reactive T-cell clones, we first performed blocking experiments that confirmed their class II restriction (figure 5A) and subsequently expressed all three potential restriction elements in the HLA class II negative HeLa cells. We observed that clones

3E1 and G44 recognized RBMX T55I within the context of HLA-DPB1*04:01, whereas T-cell clone E15 recognized the neoepitope within the context of the HLA-DP*02:01 restriction element (figure 5B). None of the clones displayed recognition of the epitope in HLA-DRB1*15:01 (online supplemental figure S4B).

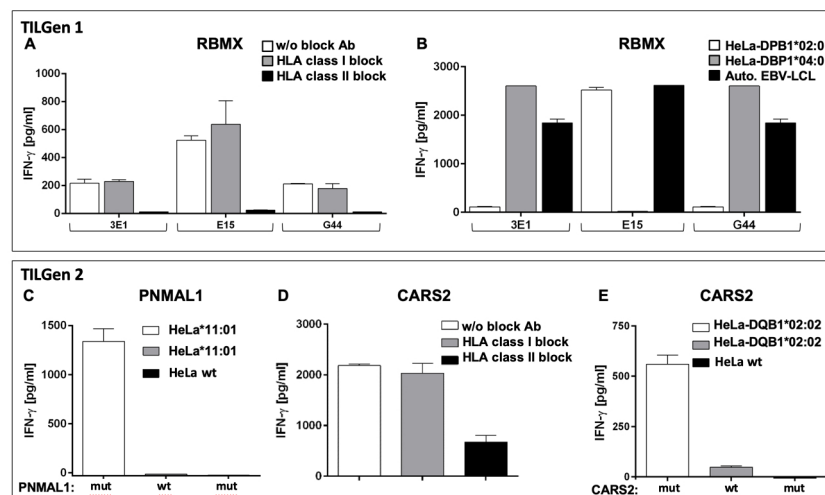


Figure 5 HLA class I or II restriction of identified neoepitopes. Blocking experiments with HLA class I and class II blocking antibodies on peptide-loaded autologous EBV-LCL confirmed restriction of the isolated (A) RBMX-specific and (D) CARS2-specific CD4+ T-cell clones to HLA class II. (B) T-cell recognition of HeLa cells retrovirally transduced with HLA-DPB1*02:01 and HLA-DPB1*04:01 was measured after loading with RBMX T55I peptide. Autologous peptide-loaded EBV-LCLs were used as controls. (C) HLA class I restricted neoepitope PNMA1 P100R was predicted to bind in HLA-A1*11:01. Loading of PNMA1 P100R peptide on HeLa cells transduced with HLA-A1*11:01 confirmed T-cell recognition in the IFN- γ ELISA. (E) T-cell recognition in IFN- γ ELISA of HLA-DQB1*02:02 transduced HeLa cells loaded with CARS2 Q171H. Shown are means and SEM of triplicates (C,D) and duplicates (A,B,E). RBMX, RNA binding motif protein X-linked; PNMA1, paraneoplastic Ma antigen family-like 1; CARS, cysteinyl tRNA synthetase 2; EBV, Epstein-Barr virus; IFN- γ , interferon gamma; LCL, lymphoblastoid cell line; TILGen, Tumor-Infiltrating Lymphocytes and Genomics.

Epitope PNMAL1 (TILGen 2) was predicted to be presented in HLA-A1*11:01, which could be confirmed by retroviral transduction of HeLa cells with this restriction molecule (figure 5C). Similarly to RBMX, the CARS2 Q171H epitope was predicted to bind to two of the patient's HLA molecules (DRB1*07:01 and DQB1*02:02). We again confirmed restriction to HLA class II by blocking studies (figure 5D) and determined HLA-DQB1*02:02 as the correct restriction molecule by retroviral transduction of HeLa cells (figure 5E and online supplemental figure S4).

Despite the technical limitations of HLA-binding prediction for HLA class II epitopes, all predicted HLA bindings could be experimentally confirmed for our identified neoepitopes.

Broadening of T-cell polyclonality is seen following treatment in TILGen 1

Chemotherapy or other treatment may affect neoantigen expression; thus, it is of interest to us to assess changes in predicted and validated neoantigens. This comparison was possible for TILGen patient 1, from whom tumor tissue was collected before and after treatment. On stimulation of TILs from the resected tumor of HER2+ TILGen 1 patient after chemotherapy with the peptide pool loaded autologous APCs, we again detected one RBMX T55I-specific T-cell clone (1A35). This T-cell clone also specifically recognized the mutated variant and was restricted to HLA-DPB1*04:01 (online supplemental figure S5A,B).

Sequencing of the TCR revealed a fourth independent clone that we had not detected at the time of diagnosis (online supplemental figure S5C). To unravel whether we missed this clone by screening of T-cell reactivities, we developed clonotypal quantitative PCRs for each of the identified clones. By this, we could show that the CDR3 regions of all four T-cell clones could be detected in the RNA of expanded T cells from the postchemotherapeutic tumor tissue. Furthermore, we could demonstrate that the CDR3 regions of the three T-cell clones isolated from core biopsy tumor tissue (prechemotherapy) could be detected in RNA of expanded T cells from peripheral blood at the time point of diagnosis, but the CDR3 of clone 1A35 could not be reliably detected at that time point (online supplemental figure S5D).

This finding suggests further induction of T-cell responses against neoepitopes in response to chemotherapy.

Neoepitopes are recognized when expressed endogenously in transduced MCF-7 BC cells

Finally, to analyze whether our newly identified epitopes could also be recognized by the T-cell clones when expressed in BC cells, we retrovirally transduced the MCF-7 human BC cell line with our full-length neoepitopes and the respective HLA molecules. We found RBMX T55I was presented both directly on MCF-7 cells and, as BC cells normally do not/rarely express HLA

class II, after exposure of EBV-LCL to antigen-expressing tumor cell lysates (figure 6A,B). In addition, because MCF-7 cells endogenously harbor the HLA-DPB1*04:01 restriction molecule of RBMX T55I, we see activation of the T-cell clones after IFN- γ induced upregulation of HLA-DP even without transduction of the HLA molecule (figure 6C,D).

To allow presentation of HLA class I-restricted antigen PNMAL1, we additionally transduced the restriction molecule HLA-A1*11:01 and tested recognition by the PNMAL1 specific T-cell clone. As depicted in figure 6E, PNMAL1 P100R and HLA-A1*11:01 positive MCF-7 cells strongly activated the respective T-cell clone.

Interestingly, we found that autologous EBV-LCLs were capable of indirectly presenting the CARS2 after pulsing with tumor cell lysates (figure 6F), but we did not observe activation of the T-cell clone by the wt antigen. However, we were not able to demonstrate direct recognition of HLA-DQB1*02:02 transduced MCF-7 cells retrovirally expressing the wt or mutated CARS2 either with or without IFN- γ pretreatment (figure 6G). Lack of T-cell recognition was not due to insufficient expression of transduced CARS2 as western blot analysis revealed strong expression (online supplemental figure S6A) and CARS2 peptide loading resulted in effective T-cell recognition, indicating sufficient expression of the HLA-DQ restriction molecule (online supplemental figure S6B).

The recognition of endogenously expressed RBMX and PNMAL1, but not CARS2, suggests the former two should be prioritized for further analysis of actionable neoantigens in patients 1 and 2, respectively. Lack of processing of endogenously expressed CARS2 might explain T-cell recognition of the exogenously loaded wt version.

DISCUSSION

The data presented herein show that by using our prediction algorithm, we can detect neoepitopes that are specifically recognized by TILs in TNBC and HER2+ patients with BC. Furthermore, these neoepitopes prove to be patient-specific both in our analysis of TCGA data as well as in our analyzed patients.

The specific targeting of tumor neoepitopes recognized by TILs and the development of individualized immune-based therapies would likely enhance checkpoint therapy, which has been disappointing as anti-PD-1 or PD-L1 monotherapy,^{5 27} and only somewhat improved by combination with atezolizumab/nab-paclitaxel. Given the rather modest mutational burden of BC,²⁸ boosting tumors to an immunologically 'hotter' state either by adoptively transferring neoepitope-specific T cells or vaccination with immunogenic neoepitopes either as adjuvant treatment after conventional chemotherapy or in combination with checkpoint inhibition has the potential to vastly improve response rates.^{29 30}

To identify actionable neoepitopes, we present here a prediction algorithm based on WGS, RNA expression data and HLA-binding prediction that allowed for successful

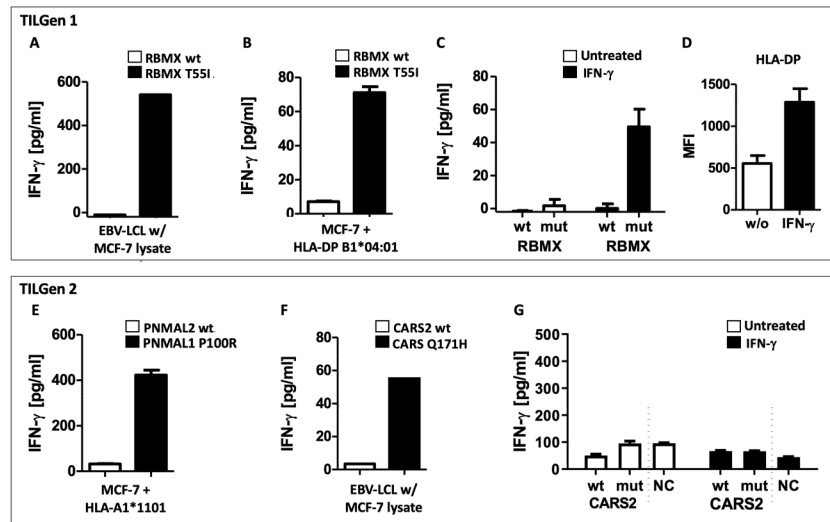


Figure 6 T-cell recognition of neopeptides expressed in MCF-7 BC cells. (A) IFN- γ ELISA of RBMX T55I-specific T cells cocultured with autologous EBV-LCL loaded with lysates of retrovirally transduced MCF-7 cells. (B) IFN- γ ELISA of T-cell recognition of MCF-7 cells retrovirally transduced with RBMX T55I or RBMX wt and the HLA-DP restriction molecule. (C) T-cell recognition as measured by IFN- γ ELISA of RBMX specific T-cell clone and RBMX T55I/wt transduced MCF-7 cells with and without prior IFN- γ treatment. (D) Surface expression of HLA-DP on MCF-7 cells with and without IFN- γ treatment as measured by flow cytometry. (E) T-cell recognition of HLA class I restricted antigen PNMAL1 P100R as well as wt variant retrovirally transduced in MCF-7 cells as measured by an IFN- γ ELISA. (F) IFN- γ ELISA of CARS2 Q171H-specific T cells cocultured with autologous EBV-LCL loaded with lysates of retrovirally transduced MCF-7 cells. (G) IFN- γ ELISA of T-cell recognition of IFN- γ treated and untreated MCF-7 cells transduced with CARS2 Q171H or CARS2 wt and the HLA-DQ restriction molecule NC: untransduced MCF-7 cells. Means with SEM of duplicates (B-E,G) are shown. BC, breast cancer; EBV, Epstein-Barr virus; IFN- γ , interferon gamma; LCL, lymphoblastoid cell line; RBMX, RNA binding motif protein X-linked; PNMAL1, paraneoplastic Ma antigen family-like 1; CARS, cysteinyl tRNA synthetase 2; Mut, mutated; NC, negative control; TILGen, Tumor-Infiltrating Lymphocytes and Genomics; wt, wild type.

identification of neoepitope-specific TILs for the first time in treatment-naïve patients with BC. In contrast to other studies,^{9 31} we purposefully included HLA-binding prediction in our algorithm to reduce the number of potential epitopes, and while this may exclude some actionable neoepitopes, specifically for high TMB tumors, it increases feasibility. In combination with the use of long overlapping peptides for potential HLA class II epitopes, HLA-binding prediction led to a reduction of potential epitopes from 143 to 28 in the first patient (18%) and from 809 to 65 in the second (8%). Although we cannot guarantee that we did not miss any neoepitope-specific response, we clearly demonstrate that this method is feasible and leads to identification of polyclonal immune responses. For patients with low mutational burden, HLA prediction can easily be excluded from the workflow. The comparison of our neoantigen prediction method to other reported methods such as MHC analysis with recurrent integrated architecture (MARIA),³² will be part of future studies.

Knowledge of both tumor and normal tissue gene sequencing is vital for accurate variant detection and the basis for accurate neoepitope predictions; our pipeline here is distinguished from others in the literature by performing such tumor:normal comparisons. The bioinformatics method used here is also highly sensitive and specific for identification of the most likely variants and filters out low-probability variants. The ranking

and prevalence of coding mutations within the dataset presented here fell within previously reported ranges that are representative of primary cancers.^{33 34}

During cancer evolution, many mutations occur and may not persist, and such mutations as well as those not in known oncogenes are likely passenger mutations. Therefore, to circumvent targeting of only certain tumor subclones, we determined the allelic frequency of any candidate target neoepitope mutation of the tumor by deep sequencing.

To further lower the risk of escape variants and to generate a sustained antitumor effect, broad targeting of both CD4+ and CD8+ T-cell neoepitopes should be used. It is therefore of note that despite technical limitations of predicting HLA class II-restricted epitopes due to the varying peptide length within the open HLA II binding groove, we were able to identify neoepitope-specific CD4+ T-cell clones in both of our analyzed patients. The deep learning-based algorithm created by Chen *et al.*³² may be a more robust approach to predicting HLA class II, and we will run a comparison in future studies. Nonetheless, our identification of these CD4+ T-cell clones allowed for combined CD4+ and CD8+-based immunotherapy. This is of particular interest as evidence has arisen that CD4+ T cells alone can actually drive therapeutic immune responses to cancer,^{35 36} including neoantigen recognition by CD4+ T cells as reported by Linnemann *et al.*³⁷ Although typically most BC cells do not express

HLA class II, the combined application of tumor-specific CD4+ and CD8+ T cells might be crucial for a sustained antitumor response. This also highlights one of the advantages of our method as compared with direct identification of neoepitopes presented on tumor cells by mass spectrometry (MS).^{38,39} While MS approaches ensure the presentation of the identified epitopes on the cell surface, their sensitivity is generally too low to identify HLA class II-restricted antigens in solid tumors as they are usually only presented on bystander APCs. MS could be used in conjunction with our method as a means to confirm presentation but not necessarily to exclude predicted neoantigens.

An additional feature of our identification protocol based on clonally expanded T cells is that it allows for direct characterization of the reactive TCR and also for clones with low initial frequencies, enabling the generation of TCR transgenic T cells for adoptive transfer.

While targeting of neoepitopes allows for high-avidity T-cell responses with a low risk of autoimmunity, induction of autoreactive antibodies^{40,41} or cross-reactivity with the wt version is possible. It is therefore advisable to test T-cell recognition of the wt version to at least avoid cross-reactivity on use of a neoepitope-based vaccine or T-cell transfer. In regard to CARS2, which shows a limited amount of cross-reactivity against the wt epitope, we suggest that for this particular antigen, discrimination between the mutated and wt antigen be determined by differential processing,^{42–44} because retroviral expression of full-length CARS2 in MCF-7 cells did not lead to T-cell recognition and exposure of APCs to tumor cell lysates resulted in specific presentation of mutant CARS2.

The neoepitopes identified here appeared to be patient-specific, and while we could find no role for CARS2 or PNMAL1 in cell proliferation or survival, RBMX plays a role in response to DNA damage. It has been reported that siRNA downregulation of RBMX decreases homologous repair to 7% of control—levels comparable to those of depletion of BRCA2.⁴⁵ Whether RBMX T551 actually influences functionality of RBMX merits further evaluation.

It has been described recently that neoadjuvant chemotherapy increases the number of stromal TILs.⁴⁶ We report here for the first time, however, the persistence and even expansion in polyclonality of a T-cell response against a defined HLA class II-restricted neoepitope during neoadjuvant chemotherapy. It would be of interest whether the general expansion of TILs consists mainly of CD4+ T cells induced by HLA class II-restricted antigens, as on tissue damage (1) tumor antigens are released and can be presented on surrounding APCs as we demonstrated for RBMX, and (2) local inflammation upregulates HLA class II expression on the tumor cells themselves, allowing direct targeting by the neoepitope-specific T cells. Besides trastuzumab and pertuzumab, the patient analyzed here was treated with docetaxel and carboplatin, a chemotherapy known to cause immunogenic cell death,⁴⁷ which

is in line with the polyclonal expansion of the immune response.

Immunotherapy clinical trials in BC have not shown clinical responses as robust as those in equivalent trials in both lung and skin cancer.²⁷ Several factors may come into play in the poor responses observed. Checkpoint inhibitor therapies are currently typically used for TMB high cancers such as melanoma or non-small cell lung carcinomas.^{48,49} In BC, there is a lower average TMB and, in general, the tumor environment is less immunogenic.²⁷ Our work has shown that there are TILs that recognize HLA-restricted neoepitopes and that they are immunologically active both in TNBC and HER+ BC. However, progressive tumor growth demonstrates the inability of these TILs to eradicate the malignant cells. Recognition of these specific personalized neoepitope sequences occurs ‘upstream’ of any potential checkpoint regulation, and any clinical use of neoepitopes may need to be combined with checkpoint inhibitors. However, patients may still benefit from immune therapy by checkpoint inhibitors in combination with cellular therapy or vaccination in a personalized fashion. This further emphasizes the need for -omics analysis in combination with the algorithm for identification of target neoepitopes described here to guide future therapies.

Author affiliations

¹Department of Internal Medicine 5, Hematology/Oncology, Friedrich-Alexander University Erlangen-Nuremberg, Erlangen, Germany

²NantHealth, Inc, Santa Cruz, California, USA

³ImmunityBio, Inc, Culver City, California, USA

⁴Department of Gynecology and Obstetrics, Friedrich Alexander University Erlangen-Nuremberg, Erlangen, Germany

⁵Department of Hematology, Leiden University Medical Center, Leiden, The Netherlands

⁶Laboratory of Tumor Immunology and Biology, Center for Cancer Research, National Cancer Institute, National Institutes of Health, Bethesda, Maryland, USA

⁷Genitourinary Malignancies Branch, Center for Cancer Research, National Cancer Institute, National Institutes of Health, Bethesda, Maryland, USA

Twitter James L Gulley @gulleyj1

Acknowledgements The authors thank all of the patients who participated in the Tumor-Infiltrating Lymphocytes and Genomics study, as well as Bettina Knörr, Silke Landrith and Sonja Öser for excellent technical assistance. We also thank Uwe Appelt, Stefanie Gross, Markus Mroz, and Dagmar Schönhofner (Core Unit Cell Sorting and Immuno-monitoring, Erlangen, Germany) for fluorescence activated cell sorting (FACS).

Contributors HR, EDvdM, JB, and SK performed all the in vitro experiments for identification of neoepitopes from patients with breast cancer; AN and JZS analyzed whole-genome sequencing and RNA-sequencing data and generated binding predictions; CJV reviewed the data; SCB supervised the analysis; KN, AM, PAF, PS-S, and ANK (with SR, MWB, and JS) conceived the study; MR coordinated the biopsy sampling and DNA isolation; AH coordinated and obtained clinical data and specimen; MG assisted with in vitro studies; JS directed the analysis at NCI; JLG advised on and reviewed the analysis; KLL assisted with in vitro studies; DHH performed in vitro studies and analyzed the data; PS-S created the figures and edited the manuscript; HR, AM, MWB, MG, PAF, and ANK wrote the manuscript.

Funding We thank the Interdisciplinary Center for Clinical Research (IZKF) (project D26 to AM and PAF) and the Wilhelm-Sander Foundation (project 2019.044.1 to ANK) for funding.

Competing interests None declared.

Patient consent for publication Not required.

Ethics approval Peripheral blood and tumor tissue were obtained after approval by the internal institutional review board and with informed patient consent according to the Declaration of Helsinki.

Provenance and peer review Not commissioned; externally peer reviewed.

Data availability statement Data are available upon reasonable request. Data have largely been presented in the text; other data are available upon request.

Supplemental material This content has been supplied by the author(s). It has not been vetted by BMJ Publishing Group Limited (BMJ) and may not have been peer-reviewed. Any opinions or recommendations discussed are solely those of the author(s) and are not endorsed by BMJ. BMJ disclaims all liability and responsibility arising from any reliance placed on the content. Where the content includes any translated material, BMJ does not warrant the accuracy and reliability of the translations (including but not limited to local regulations, clinical guidelines, terminology, drug names and drug dosages), and is not responsible for any error and/or omissions arising from translation and adaptation or otherwise.

Open access This is an open access article distributed in accordance with the Creative Commons Attribution Non Commercial (CC BY-NC 4.0) license, which permits others to distribute, remix, adapt, build upon this work non-commercially, and license their derivative works on different terms, provided the original work is properly cited, appropriate credit is given, any changes made indicated, and the use is non-commercial. See <http://creativecommons.org/licenses/by-nc/4.0/>.

ORCID iDs

Patricia Spilman <http://orcid.org/0000-0003-2626-6475>

James L Gulley <http://orcid.org/0000-0002-6569-2912>

REFERENCES

- Sampson JH, Maus MV, June CH. Immunotherapy for brain tumors. *J Clin Oncol* 2017;35:2450–6.
- Dammeijer F, Lievens LA, Veerman GDM, et al. Efficacy of tumor vaccines and cellular immunotherapies in non-small-cell lung cancer: a systematic review and meta-analysis. *J Clin Oncol* 2016;34:3204–12.
- Wang J, Reiss KA, Khatri R, et al. Immune therapy in GI malignancies: a review. *J Clin Oncol* 2015;33:1745–53.
- Pu X, Wu L, Su D, et al. Immunotherapy for non-small cell lung cancers: biomarkers for predicting responses and strategies to overcome resistance. *BMC Cancer* 2018;18:1082.
- Lyons TG, Dickler MN, Comen EE. Checkpoint inhibitors in the treatment of breast cancer. *Curr Oncol Rep* 2018;20:51.
- Santa-Maria CA, Nanda R. Immune checkpoint inhibitor therapy in breast cancer. *J Natl Compr Canc Netw* 2018;16:1259–68.
- Schmid P, Adams S, Rugo HS, et al. Atezolizumab and nab-paclitaxel in advanced triple-negative breast cancer. *N Engl J Med* 2018;379:2108–21.
- Tran E, Robbins PF, Lu Y-C, et al. T-Cell transfer therapy targeting mutant KRAS in cancer. *N Engl J Med* 2016;375:2255–62.
- Zacharakis N, Chinnasamy H, Black M, et al. Immune recognition of somatic mutations leading to complete durable regression in metastatic breast cancer. *Nat Med* 2018;24:724–30.
- North JP, Golovato J, Vaske CJ, et al. Cell of origin and mutation pattern define three clinically distinct classes of sebaceous carcinoma. *Nat Commun* 2018;9:1894.
- Neve RM, Chin K, Fridlyand J, et al. A collection of breast cancer cell lines for the study of functionally distinct cancer subtypes. *Cancer Cell* 2006;10:515–27.
- Blick T, Widodo E, Hugo H, et al. Epithelial mesenchymal transition traits in human breast cancer cell lines. *Clin Exp Metastasis* 2008;25:629–42.
- Würfel F, Erber R, Huebner H, et al. TILGen: A Program to Investigate Immune Targets in Breast Cancer Patients - First Results on the Influence of Tumor-Infiltrating Lymphocytes. *Breast Care* 2018;13:8–14.
- Erber R, Hartmann A, Beckmann MW, et al. [TILGen study-immunological targets in patients with breast cancer : Influence of tumor-infiltrating lymphocytes]. *Pathologie* 2018;39:236–40.
- Sanborn JZ, Chung J, Purdom E, et al. Phylogenetic analyses of melanoma reveal complex patterns of metastatic dissemination. *Proc Natl Acad Sci U S A* 2015;112:10995–1000.
- Teku GN, Vihinen M. Pan-cancer analysis of neopeptides. *Sci Rep* 2018;8:12735.
- Trolle T, McMurtrey CP, Sidney J, et al. The length distribution of class I-restricted T cell epitopes is determined by both peptide supply and MHC allele-specific binding preference. *J Immunol* 2016;196:1480–7.
- Lee KL, Benz SC, Hicks KC, et al. Efficient tumor clearance and diversified immunity through neopeptide vaccines and combinatorial immunotherapy. *Cancer Immunol Res* 2019;7:1359–70.
- Robinson J, Halliwell JA, Hayhurst JD, et al. The IPD and IMGT/HLA database: allele variant databases. *Nucleic Acids Res* 2015;43:D423–31.
- Lundegaard C, Lamberth K, Harndahl M, et al. NetMHC-3.0: accurate web accessible predictions of human, mouse and monkey MHC class I affinities for peptides of length 8–11. *Nucleic Acids Res* 2008;36:W509–12.
- Lundegaard C, Lund O, Nielsen M. Accurate approximation method for prediction of class I MHC affinities for peptides of length 8, 10 and 11 using prediction tools trained on 9mers. *Bioinformatics* 2008;24:1397–8.
- Jensen KK, Andreatta M, Marcatili P, et al. Improved methods for predicting peptide binding affinity to MHC class II molecules. *Immunology* 2018;154:394–406.
- Nijman HW, Houbiers JG, Vierboom MP, et al. Identification of peptide sequences that potentially trigger HLA-A2.1-restricted cytotoxic T lymphocytes. *Eur J Immunol* 1993;23:1215–9.
- Leibovitz A, Stinson JC, McCombs WB, et al. Classification of human colorectal adenocarcinoma cell lines. *Cancer Res* 1976;36:4562–9.
- Schneider M, Huber J, Hadaschik B, et al. Characterization of colon cancer cells: a functional approach characterizing CD133 as a potential stem cell marker. *BMC Cancer* 2012;12:96.
- Nagy N. Establishment of EBV-infected lymphoblastoid cell lines. *Methods Mol Biol* 2017;1532:57–64.
- Vonderheide RH, Domchek SM, Clark AS. Immunotherapy for breast cancer: what are we missing? *Clin Cancer Res* 2017;23:2640–6.
- Denkert C, von Minckwitz G, Darb-Esfahani S, et al. Tumour-infiltrating lymphocytes and prognosis in different subtypes of breast cancer: a pooled analysis of 3771 patients treated with neoadjuvant therapy. *Lancet Oncol* 2018;19:40–50.
- Fuentes-Antràs J, Guevara-Hoyer K, Balliu-Piqué M, et al. Adoptive cell therapy in breast cancer: a current perspective of next-generation medicine. *Front Oncol* 2020;10:605633.
- Liu ZB, Zhang L, Bian J, et al. Combination strategies of checkpoint immunotherapy in metastatic breast cancer. *Oncotargets Ther* 2020;13:2657–66.
- Verdegaal EME, de Miranda NFCC, Visser M, et al. Neoantigen landscape dynamics during human melanoma-T cell interactions. *Nature* 2016;536:91–5.
- Chen B, Khodadoust MS, Olsson N, et al. Predicting HLA class II antigen presentation through integrated deep learning. *Nat Biotechnol* 2019;37:1332–43.
- Schumacher TN, Schreiber RD. Neoantigens in cancer immunotherapy. *Science* 2015;348:69–74.
- Segal NH, Parsons DW, Peggs KS, et al. Epitope landscape in breast and colorectal cancer. *Cancer Res* 2008;68:889–92.
- Tran E, Turcotte S, Gros A, et al. Cancer immunotherapy based on mutation-specific CD4+ T cells in a patient with epithelial cancer. *Science* 2014;344:641–5.
- Kreiter S, Vormehr M, van de Roemer N, et al. Mutant MHC class II epitopes drive therapeutic immune responses to cancer. *Nature* 2015;520:692.
- Linnemann C, van Buuren MM, Bies L, et al. High-throughput epitope discovery reveals frequent recognition of neo-antigens by CD4+ T cells in human melanoma. *Nat Med* 2015;21:81–5.
- Bassani-Sternberg M, Bräunlein E, Klar R, et al. Direct identification of clinically relevant neopeptides presented on native human melanoma tissue by mass spectrometry. *Nat Commun* 2016;7:13404.
- Bulik-Sullivan B, Busby J, Palmer CD, et al. Deep learning using tumor HLA peptide mass spectrometry datasets improves neoantigen identification. *Nat Biotechnol* 2019;37:55–63.
- Kremer AN, van der Griendt JC, van der Meijden ED, et al. Development of a coordinated allo T cell and auto B cell response against autosomal PTK2B after allogeneic hematopoietic stem cell transplantation. *Haematologica* 2014;99:365–9.
- Joseph CG, Darrah E, Shah AA, et al. Association of the autoimmune disease scleroderma with an immunologic response to cancer. *Science* 2014;343:152–7.
- Blum JS, Wearsch PA, Cresswell P. Pathways of antigen processing. *Annu Rev Immunol* 2013;31:443–73.
- Cohen WM, Bianco A, Connan F, et al. Study of antigen-processing steps reveals preferences explaining differential biological outcomes of two HLA-A2-restricted immunodominant epitopes from human immunodeficiency virus type 1. *J Virol* 2002;76:10219–25.
- Kremer AN, Bausenwein J, Luvink E, et al. Discovery and differential processing of HLA class II-restricted minor histocompatibility antigen

- LB-PIP4K2A-1S and its allelic variant by asparagine endopeptidase. *Front Immunol* 2020;11:381.
- 45 Adamson B, Smogorzewska A, Sigoillot FD, *et al.* A genome-wide homologous recombination screen identifies the RNA-binding protein RBMX as a component of the DNA-damage response. *Nat Cell Biol* 2012;14:318–28.
 - 46 Pelekanou V, Carvajal-Hausdorf DE, Altan M, *et al.* Effect of neoadjuvant chemotherapy on tumor-infiltrating lymphocytes and PD-L1 expression in breast cancer and its clinical significance. *Breast Cancer Res* 2017;19:91.
 - 47 Hato SV, Khong A, de Vries IJM, *et al.* Molecular pathways: the immunogenic effects of platinum-based chemotherapeutics. *Clin Cancer Res* 2014;20:2831–7.
 - 48 Rizvi NA, Hellmann MD, Snyder A, *et al.* Cancer immunology. Mutational landscape determines sensitivity to PD-1 blockade in non-small cell lung cancer. *Science* 2015;348:124–8.
 - 49 Hodi FS, O'Day SJ, McDermott DF, *et al.* Improved survival with ipilimumab in patients with metastatic melanoma. *N Engl J Med* 2010;363:711–23.

DATA SUPPLEMENT

Identification and validation of expressed HLA-binding breast cancer neoepitopes for potential use in individualized cancer therapy

Hannah Reimann, Andrew Nguyen, J. Zachary Sanborn, Charles J. Vaske, Stephen C. Benz, Kayvan Niazi, Shahrooz Rabizadeh, Patricia Spilman, Andreas Mackensen, Matthias Ruebner, Alexander Hein, Matthias W. Beckmann, Edith D. van der Meijden, Judith Bausenwein, Sascha Kretschmann, Marieke Griffioen, Jeffrey Schlom, James L. Gulley, Karin L. Lee, Duane H. Hamilton, Patrick Soon-Shiong, Peter A. Fasching, Anita N. Kremer

METHODS

In vitro peptide HLA-A2 binding assay

For the determination of the *in vitro* HLA-A2 binding affinity of synthesized peptides, T2A2 cells were cultured with 50 µg/mL of the indicated peptides overnight at 37°C. The binding of exogenous peptide stabilizes the HLA-A2 complex on the surface of the TAP-deficient T2A2 cells. The affinity of the peptide to bind the HLA-A2 molecule is assessed via flow cytometry as function of increased HLA-A2 mean fluorescent intensity. FITC-labeled anti-HLA antibodies were purchased from One Lambda, and data was acquired using a FACS Calibur Flow cytometer (BD Biosciences).

In vitro generation of neoepitope-specific T cells from healthy donors

Peripheral blood from healthy donors was obtained under the appropriate Institutional Review Board (IRB) approval and with informed consent. Neoepitope-specific T cells were generated from HLA-A2 expressing healthy donor peripheral blood mononuclear cells (PBMCs) using three rounds of *in vitro* stimulation. For each round of stimulation, dendritic cells (DCs) were prepared from PBMCs by plating 2×10^7 cells/well in 6-well plates in AIM V medium (Invitrogen). Cells were allowed to adhere for 2 to 4 hours at 37°C. Following incubation, non-adherent cells were removed, and remaining cells were washed once with PBS and incubated in AIM V media containing 100 ng/mL granulocyte-macrophage colony-stimulating factor (GM-CSF; Peprotech) and 20 ng/mL interleukin-4 (IL-4; Peprotech). Cytokine-containing media was changed every 48 hours for 5 days. On day 5, DCs were matured for 1 to 2 days with CD40L (0.5 µg/mL; Enzo Life Sciences) in the presence of a cross-linking enhancer (1 µg/mL). After maturation, DCs were peptide-pulsed with MDA-MB-231 derived 9-mer neoepitopes (20 µg/mL) in RPMI media containing 10% (v/v) human AB serum for 1 hour. For the first round of *in vitro* stimulation, 2×10^6 autologous PBMCs were added per well following peptide incubation. After 48 hours, 100 ng/mL each of IL-15 (Peprotech) and IL-7 (Peprotech) were added to each well and cytokines were replenished every 2 to 3 days for 7 days. For subsequent rounds of *in vitro* stimulation, DCs were peptide pulsed for 1 hour as described above. T cells were harvested from the previous round of *in vitro* stimulation, counted, and added to new DCs in 2 mL media. IL-15 and IL-7 were added to media

every 2 days. Following the third round of *in vitro* stimulation, CD8⁺ T cells were isolated using a negative selection (Miltenyi Biotec). Purified CD8 cells rested in media containing IL-15 and IL-7 prior to assessment of either their cytotoxicity or antigen-dependent IFN- γ secretion.

Neoepitope prediction for two TILGen subjects

Preclinical validation of neoepitope prediction in BC patients

From two TILGen study^{1,2} patients, peripheral blood and tumor tissue were obtained after approval by the internal Institutional Review Board (IRB) and with informed patient consent according to the Declaration of Helsinki. Briefly, the TILGen (TILs and genomics) study was a predefined substudy of the iMODE-B (imaging and molecular detection of breast cancer) study. iMODE-B is concerned with molecular markers at the time of breast cancer diagnosis or progression, molecular detection, and imaging detection of breast cancer. The TILGen study focused on the identification of antigen-specific TILs in TNBC and HER2-positive breast cancer patients in order to identify immunogenic targets that could help to improve cancer immunotherapy. Patients were eligible for inclusion in the iMODE-B study if an indication existed for a diagnostic biopsy because of a suspicious breast lesion.^{1,2} Peripheral blood was obtained for the isolation of germline DNA and generation of antigen-presenting cells (APC) (Epstein-Barr Virus (EBV)-transformed B cells and monocyte-derived DCs). Tumor material was obtained by ultrasound guided needle-core biopsy for DNA extraction and expansion of TILs. One patient with HER2⁺ BC (TILGen 1) and another with TNBC (TILGen 2) were the initial patients tested for neoantigen-reactivity. Both received neoadjuvant chemotherapy according to standard of care and had pathological complete responses. For patient 1, resected tissue from the primary breast tumor site after neoadjuvant chemotherapy was available in addition to the initial biopsy and underwent analysis.

Generation of autologous dendritic cells (DCs)

DCs of the two breast cancer patients were generated from monocytes isolated from autologous PBMCs by magnetic separation as described in the Data Supplement. Monocytes (1×10^6 /mL RPMI) were incubated with 560 U/mL GM-CSF (Miltenyi Biotec) and 500 U/mL IL-4 (Peprotech). On day 5, 200 U/mL TNF α , 2000 U/mL IL-1 β , 1600 U/mL IL-6, 560 U/mL GM-CSF, 500 U/mL IFN- γ (all Miltenyi Biotec) and 1 μ g/ml PGE-2 (Enzo) were added. DCs were harvested on day 6 to 7 and subsequently used for stimulation.

Peptide pulsing of stimulator cells

Before pulsing, peptides were dissolved in DMSO and diluted in RPMI. Peptide pulsing was performed by incubating stimulator cells for 2 hours with synthetic peptides (1 μ g/mL or as indicated) in RPMI containing 2% human serum. Peptide-pulsed cells were washed and subsequently used as stimulator cells. Alternatively, MCF-7 cells (5×10^6 / ml RPMI) were lysed in three subsequent freeze-thawing cycles (liquid nitrogen to 37°C)

followed by loading of 100 μ L of those cell lysates onto EBV-LCLs. T-cell activation was measured either as cytokine release by IFN- γ ELISA (Invitrogen) according to the manufacturer's instructions or as upregulation of CD137 in flow cytometry. For blocking experiments, HLA class I (W6/32; Biolegend) and HLA class II (PdV5.2; Santa Cruz Biotechnology) blocking antibodies were added at 2 μ g/mL to the co-culture 30 minutes before addition of the T-cell clone.

Retroviral transduction of BC-derived neoantigens and HLA alleles

To confirm processing and presentation of neoantigens when endogenously expressed, total RNA from patient-derived EBV-LCLs was obtained using RNeasy Mini columns (Qiagen) and transcribed into cDNA by reverse transcriptase using the One Taq RT-PCR Kit (New England Biolabs, Germany). HLA restriction molecules and RBMX, PNMAL1 and CARS2 wildtype (wt) were amplified with specific primers and PNMAL1 P100R, CARS2 Q171H and RBMX T55I were generated by a 2-step PCR with oligos encoding the single nucleotide mutation (see all oligos and plasmids in Table S4). HLA-DQ and -DP α - and β - chains were fused by a T2A linker. PCR products were cloned into retroviral vector MP71 or pLZRS, including the marker genes Δ NGFR or GFP. Inserted PCR products were verified by sequencing. Wild-type ϕ nx A packaging cells were transfected with these vectors as described previously.³ Viral supernatants were used for transduction of EBV-LCL, class II negative HeLa or MCF-7 cells on plates coated with 30 μ g/ml recombinant human fibronectin CH296 (RetroNectin; Takara Bio). Expression of the transgenes was verified by marker gene expression and/or surface expression of HLA class II alleles.

Flow cytometry

For flow cytometric analysis and/or isolation of cells, the following antibodies were used: CD3 labelled with FITC or BV (Brilliant Violet) 510, APC-Cy7 or APC-labeled CD8, BV421-labelled CD4, PE-labelled CD137 and NGFR (all BD Sciences), as well as PE-labelled HLA-DP (Leinco). IFN- γ producing cells were PE-labelled by using the cytokine secretion assay (Miltenyl Biotech) followed by flow cytometric sorting (Aria II, BD). The IOTest Beta Mark TCR V β Repertoire Kit (Beckman Coulter), which enables the identification of 24 different specificities, was used to determine the T-Cell Receptor (TCR) variable beta chain of different T-cell clones.

TCR sequencing and clonotypic PCR

For TCR sequencing, RNA of T-cell clones was isolated using an RNeasy mini kit according to the manufacturer's protocol, including QIA shredder and DNase digestion (all Qiagen). cDNA was generated using SMARTScribe Reverse Transcriptase (Clontech) and 1 μ M dNTPs (Roche) with an oligo in the constant β chain region (5'-CAGTATCTGGAGTCATTGA-3') and a target switching RNA anchor with added ribosomal guanine residues (5'-AAGCAGTGGTATCAACGCAGAGTACggg-3') as described previously.⁴ In a second PCR step, amplification of the variable region was performed by using the Pwo SuperYield DNA Polymerase (Roche) according to the

manufacturer's instructions. Oligos included an anchor specific primer (5'-AAGCAGTGGTATCAACGCAGAGT-3') used in combination with a more proximal primer within the constant region (5'-CACGTGGTCGGGGWAGAAGC-3'). PCR was performed with 33 cycles, an annealing temperature of 59°C, and 1 minute of extension time. Resulting PCR bands were purified via gel electrophoresis, excised, and sequenced. Sequencing was performed using 5 µL of DNA (100 ng/µL) mixed with 5 µL of the respective primer followed by Sanger sequencing at GATC Biotech (Germany). Analysis of the resulting sequences was performed using the International Immunogenetics Information Systems.⁵

For clonotypic PCR, forward primers were designed to bind in the highly variable CDR3 region, while reverse primers bound in a distance of 70 to 120 bp. The following primers were used: 3E1 fw: 5'-CAATGGCTACAATGTCTCCAGATTAA-3', 3E1 rv: 5'-AGGCACTGCTGGCACAGA-3'; E15 fw: 5'-TCAGGGCGCCAGTTCTCTAA-3', E15 rv: 5'-CCTAAGCTGCTGGCGCAA-3'; G44 fw: 5'-CAGGAATGCCAAAGGAACGATT-3', G44 rv: 5'-CTGGTGAGCTGGCACAGAA-3'; 1A35 fw: 5'-ATCCGTCTCCACTCTGAAGATC-3', rv: 5'-TTCAGTGTTGCTCCCTAAGCT-3'. PCR was done in 10 µL reaction mix containing 100 ng of cDNA with 100 nM of each primer and 5 µL of the SYBR Select Master Mix (Thermo Scientific). Amplification was performed with 2 minutes at 50°C, 2 minutes at 95°C, followed by 65 cycles of 3 seconds at 95°C, 30 seconds at 59°C. β-Actin was used as a housekeeping gene: fw: 5'-CCGAGGACTTTGATTGCACA-3', rv: 5'-AGTGGGGTGGCTTTTAGGAT-3'. To verify specific amplification of qPCR products, they were Sanger sequenced using the described primers.

Immunoblotting

Cells (5×10^6 cells/sample) were lysed on ice in 70 µL RIPA buffer (50 mM Tris, 150 mM NaCl, 1% Triton X-100, 50 mM NaF, 0.2 mM Na₃VO₄, pH 7.4) supplemented with protease inhibitors (Roche) for 30 minutes. Cytosolic proteins were isolated from supernatants after centrifugation at 16.000 x g (20 min, 4°C) and protein concentration was determined by Pierce BCA Protein Assay Kits (Thermo Fischer Scientific). Protein lysate (15 µg) was separated by SDS-PAGE for 1 hour at 120 V using precast Mini-PROTEAN TGX 4–15% gradient gels (Bio-Rad) and blotted on 0.2 µm Trans-Blot Turbo polyvinylidene difluoride membranes (Bio-Rad). Proteins were detected by rabbit anti-CARS2 antibody (Sigma-Aldrich), mouse IgG1 anti β-Aktin (Santa Cruz), and visualized by the WesternDot 625 goat anti-rabbit Western blot kit according to the manufacturer's protocol (Life Technologies).

Table S1. HLA-A2 restricted neoepitopes identified in the MDA-MB-231 cell line. Highlighted rows indicate the 20 peptides that were synthesized for further *in vitro* analysis.

Gene Name	Transcripts per million	Affinity (nM)	Neopeptide
RTTN	6.42	6	GLQDCLHSV
PIGO	18.88	7	LLIAHFLGV
SLC17A5	29.48	9	GTIGIFWFV
MUC4	3.92	15	LLVTSLSVV
ENTPD7	4.57	23	FLRQWVAFV
PITPNM2	7.14	25	NVFDTVMHV
ARFGAP1	48.51	27	SLLPHKHVV
KIF13B	8.47	28	TLTHILYDV
RTN4	422.86	31	AMAKIQAKV
ZNF703	50.98	34	LLNPHTLGL
NCAPD3	39.7	34	YLEYGLHAA
RANBP2	35.47	35	FLTNDETGV
ADGRG6	29.04	35	SLQGLFILI
HAUS3	17.76	39	SLVQHQLAV
SLC17A5	29.48	42	GIFWVFLWI
DNAH14	10.31	45	ILIQELEEI
YIPF1	19.35	64	AMLVFAIAI
IDUA	7.58	80	LLSNDNALL
PRR16	5.21	84	SVHHYAWVV
RFX2	4.45	93	SMVGITMDI
ZCCHC7	17.23	96	NLVGYENSV
KMT2C	17.49	98	QMYHYSCAA
TCF25	38.79	99	ILCEIKEAV
ATP13A1	36.77	105	ALASCHLLM
COMMD8	26.81	116	ALSSDTIAA
MUC4	3.92	129	LLVTNASSV
DYM	12.99	130	RLLQSGAEL
PIGO	18.88	150	TMDSGEVDL
ATP11A	20.46	173	HMQDYGLII
SLC17A5	29.48	175	WFVLWIWLV
C10orf88	8.52	187	HIDDNIALL
ADAM8	87.28	191	GLLGDSSEA
IDUA	7.58	198	ALLSNDNAL
HERC2	12.92	218	LLLLQLWYS
ENTPD7	4.57	218	RQWVAFGLL
RTN4	422.86	271	KIQAKVPGL
SLC17A5	29.48	288	ILLSLRNQL
TLN1	208.07	290	KQAAHTLEA
PRDM2	12.1	320	KIQDIQLKI
USP5	53.58	360	GLGGLPNIV
COMMD8	26.81	365	KLALSSDTI
GTF3C1	29.64	385	FIGRPWHVV
PANK2	26.55	410	RLLLRMGGV
PITPNM2	7.14	415	VMHVHYPVA
DPY19L4	14.75	428	KLIASILYQ
ASPM	40.59	430	MLKPSTLII
SLC18A2	5.14	433	FANMGIALTL
YIPF1	19.35	445	WICAMLVFA
DPY19L4	14.75	464	QQMSLYPKL
RFC1	30.26	468	KQNWRLIPA

Table S2. All peptides used for screening T-cell reactivities in HER2+ TILGen patient 1 are shown. For HLA class I, all predicted neoepitopes were used as 9-mer peptides. For HLA class II, fusion peptides were generated for each mutation predicted to bind.

No.	Gene	Mutation	Sequence	HLA class	No.	Gene	Mutation	Sequence	HLA class
1	RBMX	p.T55I	SRGFAFVIF	I	21	CDK20	p.I135M	DLKPANLLMSASGQLKIADFG	II
2	RAB1B	p.L186V	RPNVKIDST	I	22	SLCO2B1	p.R369C	QFIKVFPRVLLQTLCHPIFLLVLSQVC	II
3	GOLGA3	p.H1486Tfs*35	PRGDPQRTV	I	23	ABAT	p.R450Q	DSIQNKILILIARNKGVVL	II
4	PARP9	p.G383V	LVTKVFNLF	I	24	RRN3	p.S199L	TCHRALQIIARIYVPLTPWFLMPILVEKFP	II
5	BAIAP2	p.N339K	DSYSKTLPV	I	25	FAM204A	p.D141E	WKELTQYFGVNDRFEP	II
6	PTHLH	p.D99del	FGSDEGRYL	I	26	SLC1A4	p.A516F	EETSPLVTHQNPFPGPVAS	II
7	SLC1A4	p.A516F	NFFGFPVASA	I	27	PARP9	p.G383V	AKQFQRSQLVLVTKVFNLFCKYIYHVLWH	II
8			PLVTHQNPF	I	28	RBMX	p.T55I	DRETNKSRGFAFVIFESPADAKDAA	II
9	DOK7	p.S56R	LRERSRLTL	I					
10	HELLS	p.H535R	EREKNMRSF	I					
11			RYVPLTPWF	I					
12			VPLTPWFLM	I					
13	RRN3	p.S199L	ARYVPLTPW	I					
14			YVPLTPWFL	I					
15			LLMSASGQL	I					
16	CDK20	p.I135M	MSASGQLKI	I					
17			KPANLIMSA	I					
18			LNTEMITNI	I					
19	ANAPC1	p.T416M	CIDHLWTEM	I					
20			WTEMITNIR	I					

Table S3. All peptides used for screening T-cell reactivities in TNBC TILGen patient 2 are shown. For HLA class I (left), all predicted neopeptides were used as 9-mer peptides. For HLA class II (right), fusion peptides were generated for each mutation predicted to bind.

No.	Gene	Mutation	Sequence	HLA class	No.	Gene	Mutation	Sequence	HLA class
1	HEBP2	p.F142S	RSSDGFSSA	I	27	DCUN1D2	p.D150A	LKATAKFKDQYQFTTF	II
2	DCUN1D2	p.D150A	ATAKFKDFY	I	28	SLC30A5	p.M748I	SGLSTGFHDVLAITKQMESMK	II
3	BHLHE40	p.T163S	SRDLKSSQL	I	29	IFT172	p.F1340H	FQRNMEVVLAVGHQLIGIGHSSAAEL	II
4			AKHENSRL	I	30	HEBP2	p.F142S	FIEDRAEMTVFVRSSDGFSSAQ	II
5	CARS2	p.Q171H	RVTENIFHI	I	31	FUS7	p.E223K	TKDREGKVIYAYHAA	II
6	SLC30A5	p.M748I	ITKQMESMK	I	32	BHLHE40	p.T163S	AKHENSRLKSSQLVTHLR	II
7	CSF1R	p.D698G	GYNHLEK	I	33	EMILIN2	p.K182R	KEGFQELQERKIQVLEEKVLRTR	II
8	ECI1	p.Y136D	LRLDQSNLV	I	34	GIT2	p.T309S	DAVWATQNHSAVSETTVVFLPVNFE	II
9	NUP160	p.L308V	KVRMSYKE	I	35	CARS2	p.Q171H	LPPTVILRVENIPIHSFIEGIIAR	II
10	MTMR12	p.R642H	KVWAQHYLR	I	36	CDC48	p.L202V	FRFDSRVKTFPGVTFPAAGERIY	II
11			HYLRWIFEA	I	37	DOB2	p.V164L	IKGAAMHFRYNLIVLGRY	II
12	FUS7	p.E223K	KTKDREGKK	I	38		p.V353L	PIKAAMHFRYNLIVLG	II
13	FNGAL1	p.F100R	RTQDAEFLK	I	39	MEGF8	p.G2723R	AGVATLLQLPGRHAP	II
14			DRTQDAEFL	I	40	XPO5	p.F920Y	ENYEALVSPILGPLTYLHMLRSQWQVI	II
15	TGIF1	p.M226L	RLLPDLRK	I	41	KCNK5	p.R112C	GCLFCVFTGLFGVPLC	II
16	CDC48	p.L202V	KTFGVRTFA	I	42	KIF26B	p.S553Y	DGCVFCFGHAKLGIYTI	II
17	ZNF562	p.F268C	CTNFSQLSA	I	43	NUP160	p.L308V	EHDAFIFALCQDHKVRMSYKEQMLMVA	II
18			KTKNCGKSC	I	44	ECI1	p.Y136D	AGYNKAVQELMLRLDQSNLVLVSAINGAC	II
19	PARP4	p.T1170I	LSKENSLLI	I	45	FNGAL1	p.F100R	RTQDAEFLKHLNEFL	II
20	TUT1	p.R36T	EYRTVAMAA	I	46	CARD11	p.M369I	GKDCMYKRNNTVILQEEV	II
21	ARHGAP39	p.N837S	HMDPVSOTK	I	47	TUT1	p.R36T	RWWQCLCFCRYRTVMAAVSDVE	II
22	CARD11	p.M369I	KHRMNTVIL	I	48	PCBP1	p.G52W	RIREESGARINISEW	II
23	UNKL	p.F250H	YRSTPCHSV	I	49	INTS1	p.R1657G	FGFYLLTLFTWQSSWF	II
24			RSTPCHSVK	I	50	MTMR12	p.R642H	GPEIKVWAQHYLRNIPFAQLGGG	II
25			QYRSTPCHS	I	51	USP9X	p.G2131R	AKLIVFIANFSLQDRFCPSF	II
26	AP4B1	p.T89R	LLAINRLCK	I	52	ARHGAP39	p.N837S	SYLEGYIYRMDPVSOTKGVASTYAKY	II
					53	ARHGAP39	p.N837S	GYIYRMDPVSOTKVTQHIKELLE	II
					54	FCNKL2	p.G2111A	LHDCIAEAVADTIAVV	II
					55	TEC1D9B	p.L714V	LQVALAVLDANMEQV	II
					56	ZNF562	p.F268C	GKSCNFSQLSAHAKTHK	II
					57	RAB11FIP3	p.V298L	FDEFDDFLTYEANEVTD	II
					58	AP4B1	p.T89R	APLNFDLALLAINRLCKD	II
					59	TGIF1	p.M226L	CNWFINARRLLPDLRK	II
					60	GALNS	p.C507S	GCEKLGKSLTFPESIPKKCLW	II
					61	PTEN7	p.Y239F	YDGKEKVFIAQTGGMNTVSDF	II
					62	PARP4	p.T1170I	KSLIITKSKENSLLIQTFSFAVEKRDEN	II
					63	UNKL	p.P250H	RRNPRRFQYRSTPCHSVKHD	II
					64	PPP1R13L	p.D633H	ARLNFLVLLHAALTGELEVQ	II
					65	CYP2D6	p.V370I	IHEVQRFGDIIPLGVTHMTSRDIEV	II

Table S4. All oligonucleotides and plasmids used for cloning and amplification are shown.

Construct	Cloning oligos	Sequence (5' → 3')	Plasmid	Marker gene
A1*1101	HLA 1101 For	CGCGGATCCACCATG GCCGTCATGGCGCC	pLZRS	NGFR
	HLA 1101Rev	CCGGAATTCACACTTTACAAGCTGTGAG		
DRB1*1501	HLA DRB For	CGCGGATCCACCATGGTGTGTCTGAAGCTCC	MP71	NGFR
	HLA DRB Rev	CCGGAATTCAGCTCAGGAATCCTGTTGG		
DPB1*0201	HLA DPA1 0103 For	CGCGGATCCACCATGCGCCCTGAAGACAGAATG	pLZRS	NGFR
	HLA DPA1 0103 Rev	CTCCACGTCACCGCATGTTAGAAGACTTCCTCTGCCCTCCAGGGTCCCCTGGGCCC		
	HLA DPB1 0201 For	TCTAACATGCGGTGACGTGGAGGAGAATCCCGGCCCTATGATGGTTCTGCAGGTTTCT		
	HLA DPB1 0201 Rev	CCGGAATTCCTATGCAGATCCTCGTTGAAC		
DPB1*0401	HLA DPA1 0103 For	CGCGGATCCACCATGCGCCCTGAAGACAGA ATG	pLZRS	NGFR
	HLA DPA1 0103 Rev	CTCCACGTCACCGCATGTTAGAAGACTTCCTCTGCCCTCCAGGGTCCCCTGGGCCC		
	HLA DPB1 0401 For	TCTAACATGCGGTGACGTGGAGGAGAATCCCGGCCCTATGATGGTTCTGCAGGTTTCT		
	HLA DPB1 0401 Rev	CCGGAATTCCTATGCAGATCCTCGTTGAAC		
DRB1*0701	HLA DRB1 0701 For	CGCGGATCCACCATG GTGTGTCTGAAGCTCC	pLZRS	NGFR
	HLA DRB1 0701 Rev	CCGGAATTCAGCTCAGGAATCCTGTTGG		
DQB1*0202	HLA DQA1 0201 For	CGCAGATCTACCATGATCCTAAACAAAGCTCTG	pLZRS	NGFR
	HLA DQA1 0201 Rev	CTCCACGTCACCGCATGTTAGAAGACTTCCTCTGCCCTCAAGGGCCCTTGGTGCTG		
	HLA DQB1 0202 For	TCTAACATGCGGTGACGTGGAGGAGAATCCCGGCCCTATGTCTGGAAAAAGGCTT		
	HLA DQB1 0202 Rev	CCGGAATTCAGTGCAGGAG CCCTTTC		
RBMX wt/T55I	RBMX Start For	CGCGGATCCACCATGGTTGAAGCAGATCGCC	MP71	GFP
	RBMX Stop Rev	CCGGAATCTAGTATCTGCTTCTGCCTCC		
RBMX T55I	RBMX mut For	GCTTTGTGTCATCTTTGAAAGCCAGC	MP71	GFP
	RBMX mut Rev	GGGCTTTCAAAGATGACAAAAGCAAATCC		
PNMAL wt/P100R	PNMAL Start For	CGCAGCGTCCACCATGTCCAAGACCATGGCGATG	MP71	GFP
	PNMAL Stop Rev	CGCTCGAGTCAAACCTTCTGGATTATTGGT		
PNMAL P100R	PNMAL mut For	CTGTAGAGACCGTACCCAGGATGCTGAG	MP71	GFP
	PNMAL mut Rev	CATCTGGGTACGGTCTCTACAGACCAC		
CARS wt/Q171H	CARS2 Start For	CGCAGCGTCCACCATGTTGAGGACTAC	MP71	GFP
	CARS2 Stop Rev	CGCTCGAGTCAGCCCGCTGATTTTGG		
CARS2 Q171H	CARS2 mut For	GAAAATATTCTCACATAATTTCTTTCATTG	MP71	GFP
	CARS2 mut Rev	GAAAGAAATTATGTGAGGAATATTTTCGGTTAC		

Figures and legends

Figure S1

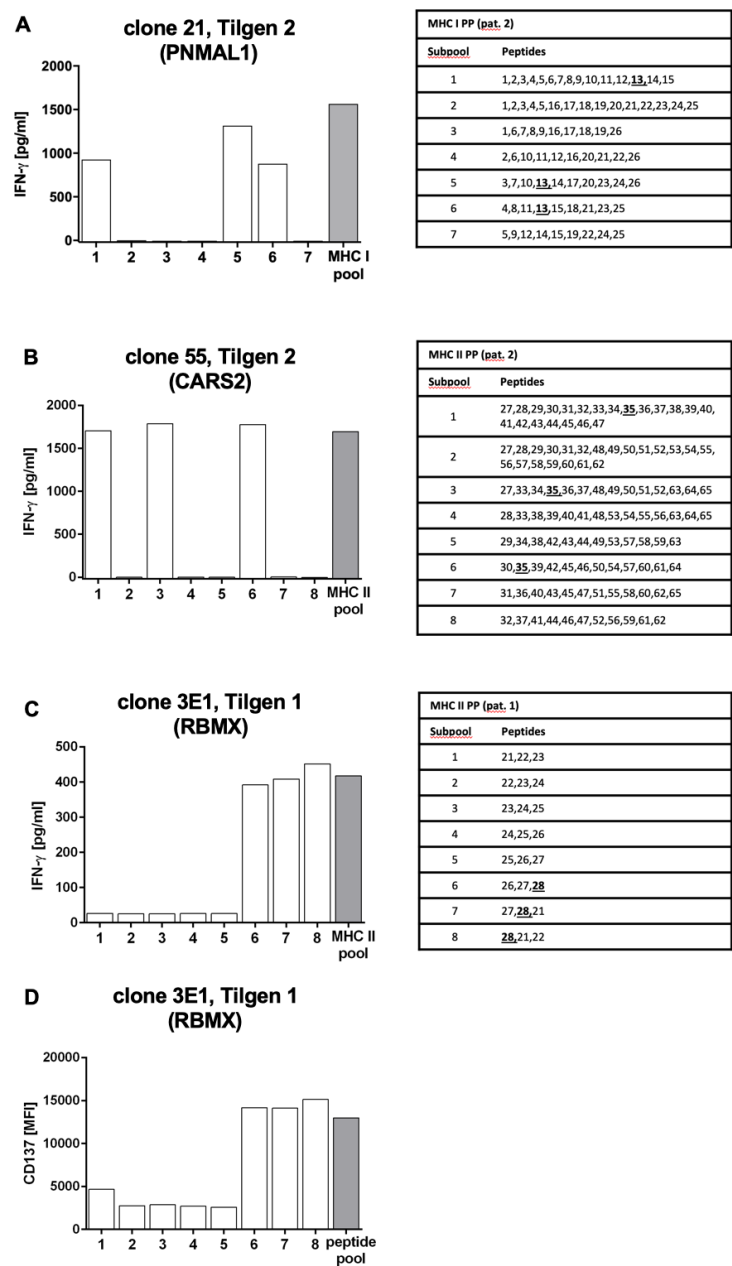


Fig. S1. Peptides of the respective MHC class I or II pool were subpooled and tested for recognition by the T-cell clones in an IFN- γ ELISA. The IFN- γ assay results are shown for (A) PNMAL1, (B) CARS2, and (C) RBMX. (D) Upregulation of CD137 as measured by flow cytometry upon peptide stimulation is shown for RBMX.

Figure S2

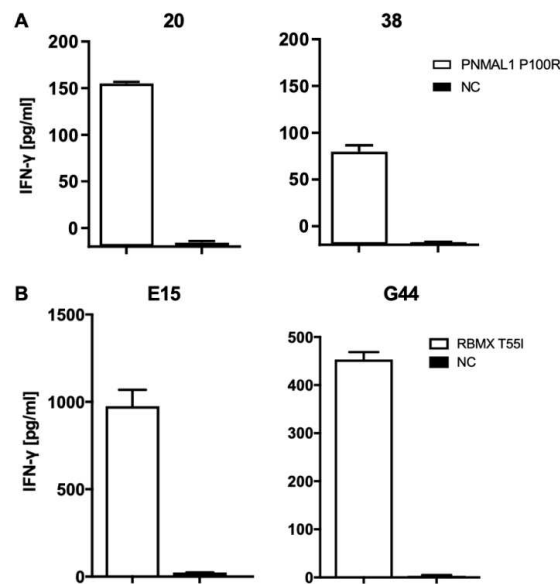


Fig. S2. Additional peptide pool reactive CD8+ T-cell clones from patient 2 (n=30) and CD4+ T-cell clones from patient 1 (n=2) were tested against PNMAL1 P100R (A) and RBMX T55I (B) peptides in an IFN-γ ELISA. For patient 2, two exemplary clones are depicted. NC (negative control): autologous EBV-LCL.

Figure S3

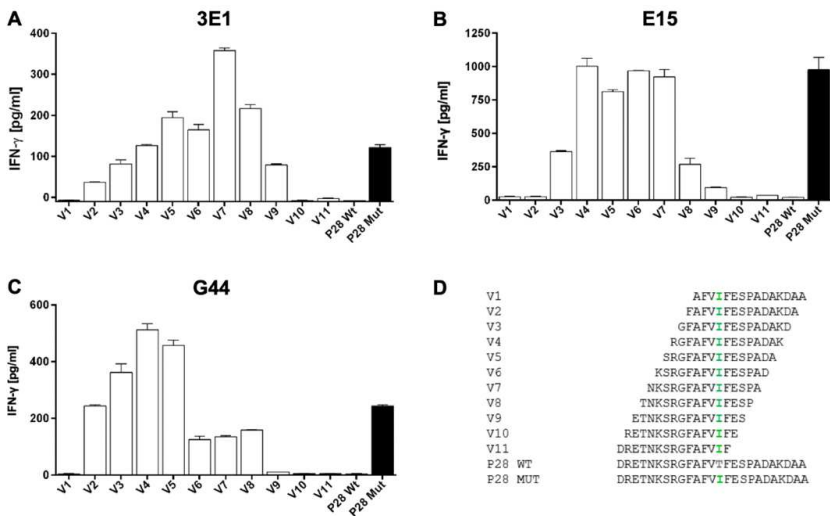


Fig. S3 The core epitope of RBMX T55I was identified for all three T-cell clones (A) 3E1, (B) E15, and (C) G44 by testing recognition of truncated peptides (D) loaded onto autologous EBV-LCL as measured in an IFN-γ ELISA. The means and SEM of duplicates are shown.

Figure S4

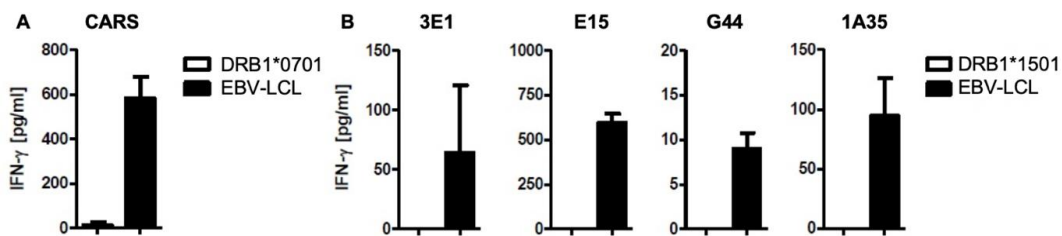


Fig. S4. T-cell recognition of HeLa cells retrovirally transduced with the predicted HLA-DRB1*0701/DRA1*0102 (A) and HLA-DRB1*1501/HLA-DRA*0102 (B). Depicted are the mean and SEM of triplicates (A) or duplicates (B) as measured after loading with CARS2 Q171H (A) and RBMX T55I (B) peptide. HLA compatible peptide-loaded EBV-LCLs were used as controls.

Figure S5

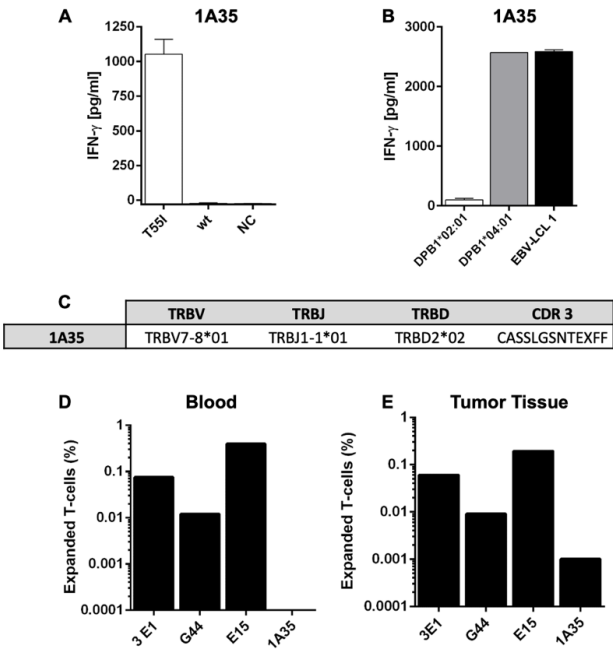


Fig. S5. RBMX T55I specific T-cell responses persist after neoadjuvant chemotherapy. (A) CD4+ T-cell clone 1A35 isolated from resected tumor tissue after neoadjuvant chemotherapy specifically recognizes RBMX T55I but not wt RBMX as measured in an IFN-γ ELISA against peptide-loaded autologous EBV-LCL from patient 1. Depicted are the mean and SEM of triplicates. NC: negative control (unloaded autologous EBV-LCL). (B) 1A35 recognizes peptide loaded HeLa cells retrovirally transduced with HLA-DPB1*0401, but not HLA-DPB1*0201 in the IFN-γ ELISA. Depicted are the mean and SEM of duplicates. (C) TCR sequencing of T-cell clone 1A35 reveals a differential variable beta chain and a unique CDR3 region. Clonotypic qPCR of all four RBMX T55I specific T-cell clones in blood (D) and tumor tissue (E) before and after neoadjuvant chemotherapy.

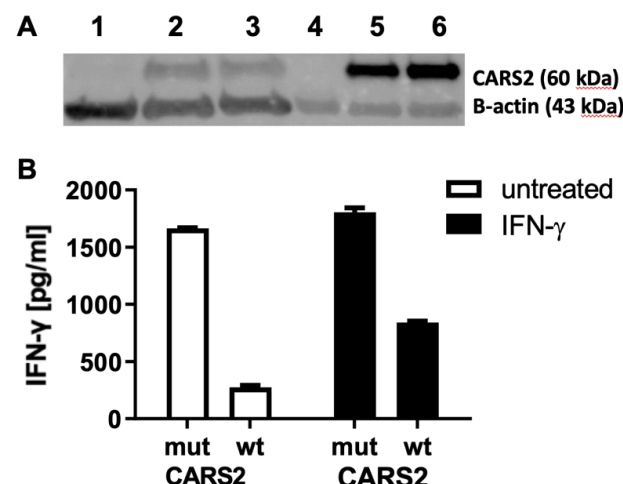
Figure S6

Fig. S6. (A) Western blot analysis of whole cell lysates of CARS2 mut/wt transduced and untransduced cells as control: 1- EBV-LCL 050; 2 - EBV-LCL 050 CARS2 mut; 3 - EBV-LCL CARS2 wt; 4 - MCF-7 wt; 5 - MCF-7 CARS2 mut; and 6 - MCF-7 CARS2 wt. Beta-actin serves as loading control. (B) T-cell recognition of CARS2 specific T-cell clone 55 of MCF-7 cell transduced with CARS2 Q171H and the HLA-DQ restriction molecule and additionally pulsed with the indicated peptide variants of CARS2 (wt or mut) as measured by IFN- γ ELISA.

References

1. Wurfel F, Erber R, Huebner H, et al: TILGen: A Program to Investigate Immune Targets in Breast Cancer Patients - First Results on the Influence of Tumor-Infiltrating Lymphocytes. *Breast Care (Basel)* 13:8-14, 2018
2. Erber R, Hartmann A, Beckmann MW, et al: [TILGen study-immunological targets in patients with breast cancer : Influence of tumor-infiltrating lymphocytes]. *Pathologe* 39:236-240, 2018
3. Griffioen M, van Egmond HME, Barnby-Porritt H, et al: Genetic engineering of virus-specific T cells with T-cell receptors recognizing minor histocompatibility antigens for clinical application. *Haematologica* 93:1535, 2008
4. Vonderheide RH, Domchek SM, Clark AS: Immunotherapy for Breast Cancer: What Are We Missing? *Clin Cancer Res* 23:2640-2646, 2017
5. Brochet X, Lefranc MP, Giudicelli V: IMGT/V-QUEST: the highly customized and integrated system for IG and TR standardized V-J and V-D-J sequence analysis. *Nucleic Acids Res* 36:W503-8, 2008